Electronic spectrum of the BF molecule[1]

R. B. Caton[2] and A. E. Douglas

Division of Pure Physics, National Research Council of Canada, Ottawa, Canada

The electronic absorption and emission spectrum of BF has been photographed at high resolution from 900 to 11 000 Å. In this work, many new electronic states have been found and corrections have been made to earlier work. The ionization potential has been determined to be between 89 635 and 89 680 cm^{-1}, with the most probable value being 89 650 cm^{-1}. Tables of the vibrational and rotational constants of all the known states of BF are presented. All but two of the excited states of BF have been classified as Rydberg states and have been assigned to Rydberg series. The interactions between the various Rydberg states are discussed.

A. Introduction

The emission spectrum of the BF molecule is readily excited and has been investigated in considerable detail. Robinson (1963) carried out an extensive investigation of the singlet band systems and has summarized earlier work. Barrow, Premaswarup, Winternitz, and Zeeman (1958), hereafter referred to as BPWZ, have published rotational analyses of two triplet systems and, since then, two additional investigations of triplet systems have been reported by Czarny and Felenbok (1968) and by Krishnamachari and Singh (1965). Also, since BF is a member of the interesting isolectronic group of molecules N_2, CO, and BF, several detailed theoretical calculations of the characteristics of the ground and excited states have been carried out. The ground state and valence states have been studied in detail by Nesbet (1964, 1965) and by Huo (1965) and the Rydberg states have been treated by Lefebvre-Brion and Moser (1965a). In spite of these numerous investigations, the absorption spectrum has not been observed, the assignment of many of the electronic states is uncertain, the analysis of some of the band systems is doubtful, and the ionization potential and the dissociation energy are only poorly determined.

In the present work, we have photographed the absorption spectrum from the visible down to 900 Å and the emission spectrum from 1200 to 11 000 Å. The new spectra show many new band systems, including a Rydberg series which approaches a series limit. A number of errors in the earlier work have been corrected and the assignment of the electronic states has been greatly clarified. Most previous results have been incorporated into tables to give a comprehensive survey of all data on the BF molecule. The new results are compared with recent theoretical calculations.

B. Experimental

The spectrum of BF was obtained, in absorption, following a flash discharge through BF_3 mixed with either Ar or He. The apparatus has been described elsewhere by Herzberg and Lagerqvist (1968). Briefly, a 0.05 μF condenser is charged to approximately 12 kV and then discharged through an absorption tube containing the gas mixture. After a short time delay, the absorption spectrum of the gas is photographed using a Lyman-type flash lamp as the light source. The BF molecule has a relatively long life and could be observed for several hundred milliseconds after the condenser was discharged. In all experiments, the Ar or He pressure was about 10 Torr and the BF_3 pressure, which was varied and never measured accurately, was only a small fraction of 1 Torr.

The absorption spectrum was photographed with a 10.7 m concave grating spectrograph (Douglas and Potter 1962). In the 1180–2000 Å region, where a foreprism and an absorption tube with LiF windows were used, the spectrum was photographed in the sixth to the ninth orders of a 600 groove per mm grating. Iron lines from a neon-filled, iron hollow-cathode lamp were photographed in overlapping orders as wavelength standards.

---

[1] NRCC No. 11048.

[2] National Research Council of Canada Postdoctoral Fellow 1967–69. Present address: Division of Science, Scarborough College, University of Toronto, West Hill, Ontario.
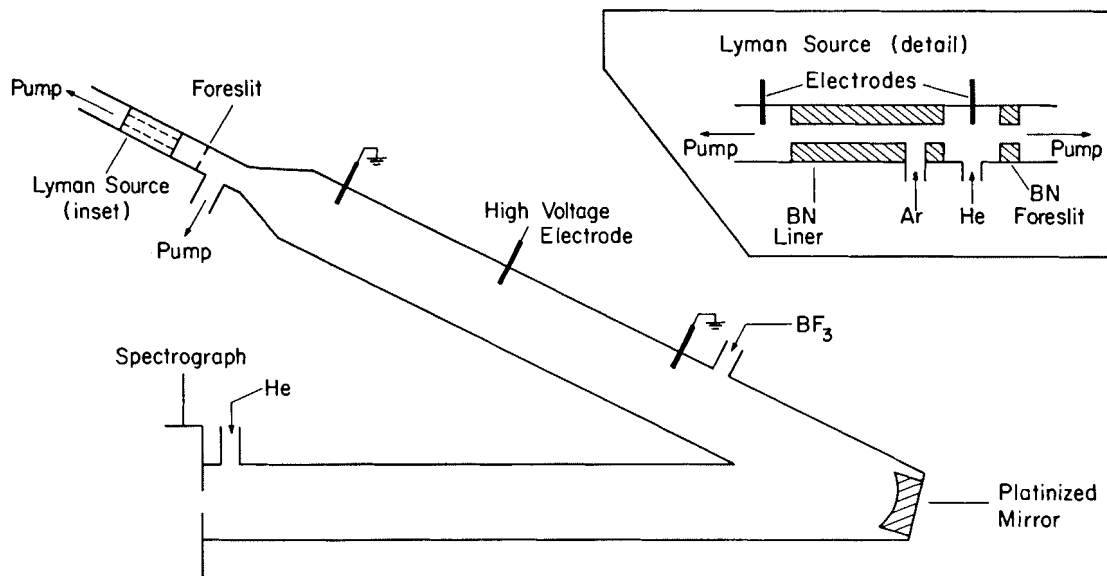
FIG. 1. Schematic diagram of the windowless flash discharge apparatus. The BF_3 is decomposed to give BF by the discharge of a condenser between the high-voltage electrode and the two ground electrodes. The details of the Lyman source, which are omitted on the large diagram, are shown in the inset diagram. Argon, rather than helium, is necessary in the Lyman source to obtain sufficient intensity.

For the absorption studies, Matheson C.P. grade BF_3 having a nominal purity greater than 99.5% was used without further purification. In some experiments BF_3 enriched in the ^{10}B isotope was used. This isotopically enriched BF_3 was obtained by the thermal decomposition of $CaF_2 \cdot BF_3$ which was obtained from the Oak Ridge National Laboratory and was stated to have an atomic isotope composition of 95.96% ^{10}B.

Although time delays between the flash discharge and the Lyman source flash varied from a few microseconds to 200 ms, most photographs were taken with a time delay of 10 ms. With a 10 ms delay, the BF was vibrationally and rotationally cool and there is very little absorption from the $v'' = 1$ and higher vibrational states. The only impurity bands which appeared in the spectrum were due to CO and occasionally BO.

Below 1180 Å where the LiF windows and fore-prism are opaque, the spectrum was photographed in the first order of a 1200 grooves per mm grating with the same spectrograph. The apparatus is shown in Fig. 1. The flow of gas in the apparatus was controlled such that the Lyman source contained largely Ar but there was little Ar between the spectrograph and the source.

The pressure in the Lyman source was about 80 Torr. The gas flow also prevents the BF_3 and its decomposition products from contacting the mirror. The absorption chamber was pumped by a 20 l/s mechanical pump so that a pressure of about 7 Torr was maintained in the volume between the boron nitride foreslit and the spectrograph slit. The configuration shown in Fig. 1 produces a stigmatic image of the Lyman source on the photographic plate of the spectrograph. On the first-order plates, absorption and emission lines of impurities were used as wavelength standards.

No bands of BF_3 were observed in any of the experiments, but continuous absorption of BF_3 made the experiments difficult in the short-wavelength region. By limiting the amount of BF_3 in the absorption tube and destroying most of it by the discharge, we were able to obtain absorption spectra of BF. The resolution of the first-order spectra is insufficient to allow a rotational analysis of the bands and thus, below 1180 Å, only band heads were measured.

BF emission was produced in a flowing mixture of BF_3 with He by either a 2450 MHz microwave discharge or a DC discharge in an aluminum hollow cathode. Impurities in the cylinder BF_3

were removed by alternate freezing and pumping, and subsequently the BF_3 was stored in a Pyrex bulb. In order to reduce impurity emission to a minimum, the microwave discharge was confined to a tube made of boron nitride. Practically no BO emission appeared in the spectrum of this discharge, in contrast to the spectrum of a similar discharge in a quartz tube which is dominated by BO emission throughout the ultraviolet and visible. Spectra in the region from 1200 Å to 11 000 Å were photographed with either a 10.7 m vacuum spectrograph or a 6 m spectrograph. The comparison spectrum was again that of a neon-filled, iron hollow-cathode lamp.

C. Results

The results and discussion are presented in Sections C, D, and E. Readers interested in the properties of BF will find all the results in Sections C and E. Section D gives a detailed description of the spectrum and its analysis.

C(1) General Comments, Observations, and Molecular Constants

The spectrum of BF, both in emission and absorption, is characterized by a large number of bands, almost all of which are free from perturbations and are readily analyzed. In this respect, it differs greatly from the spectra of CO, N_2, and NO where strong interactions between the higher electronic states lead to many local vibrational and rotational perturbations. As will be discussed in Section E, strong interactions certainly do exist in BF, but the energy differences between the states and the shapes of the potential curves are such that the interactions show up only as somewhat anomalous B and D values and do not complicate the vibrational and rotational analyses.

The analysis of the bands was carried out by the traditional graphical method to determine band origins and rotational constants (Herzberg 1950). Subsequently, the bands were fitted by a least-squares computer program provided by Dr. J. W. C. Johns. The rotational energy levels of all states could be fitted satisfactorily using terms to second order in $J(J + 1)$. In virtually every case, the results of the graphical analysis agreed with those of the least-squares fit. The best rotational energy levels of the $v = 0$ level of the ground state of BF were obtained by a least-squares fit to 270 unweighted combination differences (with J

values up to 27) from well-resolved absorption bands. The ground-state energy levels were then held fixed, and all upper-state levels were determined relative to them. Emission bands were fitted by the same procedure, allowing variation of both upper- and lower-state constants to second order in $J(J + 1)$.

All the electronic states of BF except the ground state and the lowest excited singlet and triplet states have been assigned as Rydberg states. The Rydberg states are formed from a BF^+ core, which is in a $^2\Sigma$ state, and an electron which can be characterized by values of n, l, and λ [$(4s\sigma)$, $(5p\pi)$, etc.]. The Λ value for a Rydberg state is therefore the same as the λ value of the outer electron and it has proved convenient to designate the singlet Rydberg states by the symbols characterizing the excited electron. It will be shown later that there is a considerable mixing of states and that these symbols have no exact meaning. They nevertheless are a convenient set of symbols which, to a certain approximation, do characterize the states. The triplet states which are fewer in number, and not so readily understood, have been designated in the usual way by letters of the alphabet and Λ values.

The correlation between the symbols used to denote the states here and those used by earlier workers is given in Table I. This correlation also involves some corrections to the earlier assignments. The wavelengths and the assignments of all the observed band heads of BF are given in Table II and the constants which we have

TABLE I

Nomenclature in the previous and present work

Robinson*	Previous authors	Present authors
$A^1\Pi$	$A^1\Pi$†‡	$A^1\Pi$
$B^1\Sigma$	$B^1\Sigma$†‡	$(3s\sigma)$
$C^1\Sigma$	$C^1\Sigma$†‡	$(3p\sigma)$
	$D^1\Pi$†‡	$(3p\pi)$
$E^1\Sigma$		$(3d\delta)$
$G^1\Sigma$	$E^1\Sigma$‡	$(4s\sigma)$
$F^1\Sigma$		$(3d\pi)$
$D^1\Pi$		$d^3\Pi$
$J^1\Sigma$	$e^3\Sigma$§	$e^3\Sigma$
$H^1\Sigma$	$b^3\Sigma$§‖	$b^3\Sigma$
	$a^3\Pi$‖	$a^3\Pi$
	$c^3\Sigma$‖	$c^3\Sigma$

*Robinson (1963).
†Chrétien (1950).
‡Mal'tsev (1960).
§Czarny and Felenbok (1968).
‖Barrow et al. (1958); Krishnamachari and Singh (1965).

TABLE II

Observed band heads of ^{11}BF

			Singlet–singlet transitions				
λ^{vac}	Electronic transition	Vibrational transition	Comments	λ^{vac}	Electronic transition	Vibrational transition	Comments
2085.7	$A–X$	4–6	Q,r,a,b	1162.8	(6pπ)–X	0–0	P,v
2084.4	,,	,,	R,r,a,b	1162.5	,,	,,	Q,v
2080.8	,,	3–5	Q,r,a,b	1150.7	(7pσ)–X	0–0	P,v
2079.4	,,	,,	R,r,a,b	1149.8	?	?	
2076.3	,,	2–4	Q,r,a,b	1148.9	(7pπ)–X	0–0	v
2074.8	,,	,,	R,r,a,b	1148.2	(5pσ)–X	2–0	P,v
2072.1	,,	1–3	Q,r,a,b	1143.4	(6pσ)–X	1–0	P,v
2070.5	,,	,,	R,r,a,b	1142.8	?	?	D
2038.1	,,	5–6	Q,r,a,b	1142.5	?	?	D
2037.1	,,	,,	R,r,a,b	1141.6	(8pσ)–X	0–0	D
2032.1	,,	4–5	Q,r,a,b	1140.5	(8pπ)–X	0–0	D
2031.1	,,	,,	R,r,a,b		(6pπ)–X	1–0	D
2026.5	,,	3–4	Q,r,a,b	1135.7	(9pσ)–X	0–0	D
2025.4	,,	,,	R,r,a,b	1134.8	(9pπ)–X	0–0	D
2021.3	,,	2–3	Q,r,a,b	1130.9	(10pπ)–X	0–0	D
2020.2	,,	,,	R,r,a,b	1129.0	(7pσ)–X	1–0	P,v
2016.4	,,	1–2	Q,r,a,b	1128.1	(11pπ)–X	0–0	D
2015.2	,,	,,	R,r,a,b	1127.1	?	?	D
2011.7	,,	0–1	Q,r,a,b	1127.0	(7pπ)–X	1–0	D
2010.5	,,	,,	R,r,a,b	1126.0	(12pπ)–X	0–0	D
1968.3	,,	2–2	Q,r,a,b	1124.3	(13pπ)–X	0–0	D
1963.6	,,	,,	R,r,a,b	1123.0	(14pπ)–X	0–0	D
1962.7	,,	1–1	Q,r,a,b	1122.3	?	?	D
1961.8	,,	,,	R,r,a,b	1122.0	(15pπ)–X	0–0	D
1957.39	,,	0–0	Q,r,c,b	1121	?	?	D
1956.52	,,	,,	R,r,c	1120.2	(8pσ)–X	1–0	D
1911.04	,,	1–0	Q,r,c	1119.3	(8pπ)–X	1–0	D
1910.35	,,	,,	R,r,c	1118.3	?	?	D
1867.78	,,	2–0	Q,r,c	1114.4	(9pσ)–X	1–0	D
1867.23	,,	,,	R,r,c	1113.6	(9pπ)–X	1–0	D
1827.42	,,	3–0	Q,r,c	1110.7	?	?	D
1826.95	,,	,,	R,r,c	1110.0	(10pπ)–X	1–0	D
1527.13	(3sσ)–X	0–0	P,v,c	1107.8	?	?	D
1489.25	,,	1–0	P,v,c	1107.1	(11pπ)–X	1–0	D
1453.73	,,	2–0	P,v,c	1105.0	(12pπ)–X	1–0	D
1446.91	(3pσ)–X	0–0	P,v,c	1103.5	(13pπ)–X	1–0	D
1414.58	,,	1–0	P,v,c	1102.2	(14pπ)–X	1–0	D
1384.27	,,	2–0	P,v,c	1101.8	?	?	D
1383.80	(3pπ)–X	0–0	P,v,c	1101.2	(15pπ)–X	1–0	D
1383.39	,,	,,	Q,v,c	1100.4	(16pπ)–X	1–0	D
1352.76	,,	1–0	P,v,c	1099.8	(17pπ)–X	1–0	D
1352.29	,,	,,	Q,v,c	1099.2	(18pπ)–X	1–0	D
1297.51	(4sσ)–X	0–0	P,v,c	λ^{air}			
1289.84	(3dπ)–X	0–0	P,v,c	8620.2	(4sσ)–(3sσ)	0–0	r,b,d,e
1272.07	(3dσ)–X	0–0	P,v,c	8364.8	(3sσ)–A	0–2	P,v,b,e
1269.85	(4sσ)–X	1–0	P,v,c	8038.5	(3sσ)–A	1–3	P,v,f
1254.02	(4pσ)–X	0–0	P,v,c	7595.3	,,	0–1	P,v,f
1239.70	(4pπ)–X	0–0	P,v,c	6942.1	,,	0–0	P,v,b,e
1239.43	,,	,,	Q,v,c	6414.2	(3pσ)–A	0–2	P,v,f
1228.78	(4pσ)–X	1–0	P,v,c	6221.0	(3sσ)–A	1–0	P,v,b,e
1214.55	(4pπ)–X	1–0	P,v,c	5951.6	(3pσ)–A	0–1	P,v,f
1214.24	,,	,,	Q,v,c	5644.7	(3sσ)–A	2–0	P,v,f
1210.46	(5sσ)–X	0–0	P,v,c	5543.0	(3pσ)–A	0–0	P,v,b,e
1204.91	(4pσ)–X	2–0	P,v,c	5172.2	(3sσ)–A	3–0	P,v,f
1193.35	(5pσ)–X	0–0	P,v,c	5098.6	(3pσ)–A	1–0	P,v,f
1187.68	(5pπ)–X	0–0	P,v,c	4876.5	(3dδ)–A	0–4	P,v,c
1187.43	,,	,,	Q,v,c	4617.1	,,	0–3	P,v,f
1182.4	?	?		4377.9	,,	0–2	P,v,f
1182.0	?	?		4166.3	(3dπ)–A	0–2	P,v,e
1174.4	(6sσ)–X	0–0	P,v	4157.7	(3dδ)–A	0–1	P,v,e
1170.2	(5pσ)–X	1–0	P,v	3966.2	(3dπ)–A	0–1	P,v,c
1165.7	(6pσ)–X	0–0	P,v	3953.9	(3dδ)–A	0–0	P,v,c
1164.5	(5pπ)–X	1–0	P,v	3780.2	(3dπ)–A	0–0	P,v,e
1164.3	,,	,,	Q,v				

TABLE II (*Concluded*)

λ^{air}	Electronic transition	Vibrational transition	Comments	λ^{air}	Electronic transition	Vibrational transition	Comments
10293.9	*d–b*	0–0	Q,v,c,b	6709.8	*e–b*	0–0	v,c,d,b,h
10199.5	"	1–1	Q,v,c	6678.6	"	1–1	v,c,d
10084.2	"	2–2	Q,v,c	6095.8	*f–b*	0–0	Q,v,c
9939.8	"	3–3	Q,v,c	6061.4	"	1–1	Q,v,c
9757.0	"	4–4	Q,v,c	5905.8	*g–b*	0–0	v,c,d
9586.7	*f–c*	0–0	Q,v,c	5200.0	*h–b*	0–0	Q,v,c
9462.2	"	1–1	Q,v,c	5174.6	"	1–1	Q,v

Triplet–triplet transitions[g]

NOTE: ^{R}, ^{Q}, and ^{P} indicate the type of branch. ^{r} and ^{v} indicate red or violet shading. ^{D} indicates a diffuse head.
[a] Onaka (1957).
[b] Rotationally analyzed by other authors.
[c] Rotationally analyzed by present authors.
[d] λ_0.
[e] Robinson (1963).
[f] Approximate measurement by present authors.
[g] Pearse and Gaydon (1963) list the strong heads of the *b–a* and *c–a* systems.
[h] Czarny and Felenbok (1968).

determined from the rotational analysis of a number of these bands are given in Table III. In Table IV, the constants for the electronic states are presented. All of the observed singlet and triplet states are shown in the energy-level diagrams in Figs. 2 and 3.

As shown in Table II, there is, near 1100 Å, an important set of bands which has allowed us to determine the ionization potential. There are two progressions of bands which prove to be the 0–0 and 1–0 bands of a Rydberg series. The progressions converge at 89 650 and 91 330 cm^{-1}. The resolution is insufficient to allow rotational analyses of these bands; the relationship between the features we have measured and the band origins is uncertain. We believe the true series limit of the 0–0 bands and hence the ionization potential of BF to lie between 89 680 and 89 635 cm^{-1}, with 89 650 cm^{-1} being the most probable value.

D. Band Systems of BF

In this section we discuss the characteristics of each of the band systems. Readers interested only in the results may omit this section and turn to Section *E*.

An appendix giving the wave numbers of the observed spectral lines has been placed in the Depository of Unpublished Data.[3] This appendix

[3]Photocopies of material in the depository may be obtained free of charge, upon request, from: Depository of Unpublished Data, National Science Library, National Research Council of Canada, Ottawa 7, Canada.

shows the observed vacuum wave numbers of the lines and the wave numbers calculated from the constants given in Table III.

D(1) The Ground State $X^1\Sigma^+$

The combination differences $\Delta_2 F(J)$ of the ground state were determined from many bands. The values of 270 combination differences were fitted by a least-squares method to give the ollowing rotational constants:

$$B_0 = 1.5075 \pm 0.0006 \text{ cm}^{-1}$$

$$D_0 = (7.57 \pm 0.67) \times 10^{-6} \text{ cm}^{-1}$$

All the *B* and *D* values of excited singlet states are determined relative to these values.

The B_0 given above does not agree well with that given by Onaka (1957) but, as Calder and Ruedenberg (1968) have pointed out, Onaka's value is unreliable. The B_e, α_e, and γ_e values given in Table IV were obtained from a re-evaluation of Onaka's results with the substitution of our B_0 value. These constants agree well with those predicted by Calder and Ruedenberg.

D(2) The $A^1\Pi–X^1\Sigma$ System

The $A^1\Pi–X^1\Sigma$ system can be observed either in emission or in absorption. Onaka (1957) has studied the system in emission and we have measured the absorption bands. Since the absorption bands are free from overlapping sequence bands which are troublesome in emission (our resolution appears to be somewhat better than that obtained by Onaka), we believe the rotational

TABLE III

Constants from the rotational analyses of individual bands (cm^{-1})

System	$(v'-v'')$	ν_0	$B'(RP)$	$B'(Q)$	$D'(RP)$ $(\times 10^6)$	$D'(Q)$ $(\times 10^6)$	B''	D'' $(\times 10^6)$	σ^b	Comments
$A-X$	(0–0)	51088.66(2)^a	1.4135(2)	1.4139(2)	6.87(21)	7.69(42)	1.5075(6)^c	7.57(67)^c	0.10	
	(1–0)	52327.92(2)	1.3947(2)	1.3949(2)	7.96(42)	8.01(48)	,,	,,	0.08	
	(2–0)	53539.72(3)	1.3751(4)	1.3752(3)	8.41(81)	7.87(51)	,,	,,	0.12	
	(3–0)	54722.84(3)	1.3547(2)	1.3549(2)	8.21(33)	8.06(22)	,,	,,	0.13	
$(3s\sigma)-X$	(0–0)	65499.42(3)	1.6502(2)		7.58(35)		,,	,,	0.10	
	(1–0)	67167.72(3)	1.6322(2)		6.58(25)		,,	,,	0.14	
	(2–0)	68810.81(5)	1.6144(5)		5.73(102)		,,	,,	0.18	
$(3p\sigma)-X$	(0–0)	69135.19(5)	1.6141(2)		7.29(25)		,,	,,	0.17	
	(1–0)	70719.29(3)	1.5946(2)		6.98(24)		,,	,,	0.11	
	(2–0)	72274.39(3)	1.5753(3)		6.87(45)		,,	,,	0.13	
$(3p\pi)-X$	(0–0)	72286.06(5)	1.6201(7)	1.6192(7)	6.22(159)	6.42(159)	,,	,,	0.17	
	(1–0)	73948.02(5)	1.6031(6)	1.6023(6)	5.57(123)	5.87(126)	,,	,,	0.17	
$(4s\sigma)-X$	(0–0)	77096.41(4)	1.5980(4)		1.17(57)		,,	,,	0.13	
	(1–0)	78782.04(7)	1.5833(8)		22.76(142)		,,	,,	0.22	
$(3d\pi)-X$	(0–0)	77542.79(15)	1.6934(4)	1.6511(5)	10.91(16)	6.81(34)	,,	,,	0.50	
$(3d\sigma)-X$	(0–0)	78691.21(10)	1.6511(3)		13.02(303)		,,	,,	0.32	
$(4q\sigma)-X$	(0–0)	79763.28(3)	1.6294(2)		6.42(17)		,,	,,	0.11	
	(1–0)	81404.43(8)	1.6122(6)		6.23(73)		,,	,,	0.31	
	(2–0)	83020.45(5)	1.5946(3)		6.10(39)		,,	,,	0.22	
$(4p\pi)-X$	(0–0)	80681.98(6)	1.6465(8)	1.6405(7)	7.04(168)	5.86(124)	,,	,,	0.20	
	(1–0)	82355.07(8)	1.6299(12)	1.6248(10)	9.33(299)	7.32(243)	,,	,,	0.21	
$(5s\sigma)-X$	(0–0)	82650.21(4)	1.5578(7)		−21.30(228)		,,	,,	0.11	
$(5p\sigma)-X$	(0–0)	83817.71(6)	1.6275(6)		5.63(87)		,,	,,	0.22	
$(5p\pi)-X$	(0–0)	84218.92(9)	1.7624(12)	1.7478(9)	7.39(293)	7.04(132)	1.6025(6)	8.55(67)	0.36	d
$(3d\delta)-A$	(0–0)	25295.69(1)	1.6212(4)		6.49(31)		1.4137(4)	7.09(31)	0.04	e
	(0–4)	20508.25(1)	1.6205(3)		6.21(34)		1.3328(3)	7.49(30)	0.03	e
$d-b$	(0–0)	9711.65(1)	1.6434(4)	1.6423(4)	6.50(48)	6.46(42)	1.6282(3)	6.98(42)	0.03	
	(0–0)	9712.80(2)	1.7471(12)		8.01(183)		1.7308(11)	8.51(156)	0.07	d
	(1–1)	9801.58(1)	1.6263(6)	1.6251(6)	6.86(60)	6.78(69)	1.6056(6)	7.56(69)	0.05	
	(2–2)	9914.01(1)	1.6094(3)	1.6083(3)	6.03(40)	5.96(46)	1.5811(3)	7.18(46)	0.02	
	(3–3)	10057.78(1)	1.5931(6)	1.5920(7)	6.11(174)	5.65(213)	1.5537(7)	7.41(213)	0.03	
	(4–4)	10246.20								g
$e-b$	(0–0)	14899.56(1)	1.6371(2)		6.32(8)		1.6277(2)	6.79(8)	0.04	f
	(1–1)	14969.08(3)	1.6220(9)		5.71(78)		1.6050(9)	6.19(87)	0.09	f
$f-c$	(0–0)	10428.15(5)	1.6273(20)	1.6562(20)	4.15(177)	5.49(171)	1.6030(20)	5.54(159)	0.22	h
	(1–1)	10565.0(1)								
$f-b$	(0–0)	16400.10(1)	1.6271(4)	1.6560(4)	4.51(33)	6.01(30)	1.6267(3)	6.17(30)	0.03	
	(1–1)	16493.4(3)								
$g-b$	(0–0)	16927.59(3)	1.6765(20)		5.12(540)	6.59(354)	1.6273(18)	4.07(520)	0.09	
$h-b$	(0–0)	19225.28(2)	1.6487(12)	1.6463(12)	5.82(324)		1.6278(12)	7.32(354)	0.05	
	(1–1)	19319.7								

^{a}Numbers in parentheses ( ) are three times the standard deviation of a least-squares fit.
$^b\sigma$ is three times the standard deviation of the (observed–calculated) residuals in the line fit.
^{c}Computed from 270 unweighted values of $\Delta_2 F''$.
^{d}B^{10}F.
$^e\Lambda$ doubled Q lines averaged for calculation of constants.
^{f}F$_2$ components.
$^g B'(Q) - B''(Q) = 0.0557$; $D'(Q) - D''(Q) = 2.32 \times 10^{-6}$.
$^h B'(Q) - B''(Q) = 0.0569$.

TABLE IV

Molecular constants of the ¹¹BF molecule

State	$T_0{}^b$	$\omega_e{}^c$	$\omega_e x_e$	$B_e{}^{d,e}$	α_e	D_0 $(\times 10^6)$	$r_e{}^f$ $(\times 10^8$ cm$)$	Observed transitions Designation	ν_{00}
$h^3\Pi$	$x+51265.70$	(1679.2)		(1.647_5)		6.2	(1.211_8)	$h\to b$	V 19225.28
$g^3\Sigma^+$	$x+48968.01$			(1.676_5)		5.1	(1.201_3)	$g\to b$	V 16927.59
$f^3\Pi$	$x+48440.3$	(1677.7)		(1.641_6)		5.0	(1.214_0)	$f\to b$ / $f\to c$	V { 16400.10 / 10428.15 }
$e^3\Sigma^+$	$x+46939.98$	(1654.29)		1.644_7	0.0151	6.3	1.212_9	$e\to b$	V 14899.56
$d^3\Pi$	$x+41752.06$	1696.81	11.0	1.6518	0.0176^g	6.5	1.2103	$d\to b$	V 9711.65
$c^3\Sigma^+$	$x+38011.97^h$	(1540.7)		(1.603_0)		5.5	(1.228_5)	$c\to a$	V 38011.97^h
$b^3\Sigma^+$	$x+32040.42^h$	1629.28^h	22.255^h	1.6385	0.0200^i	6.3	1.2151	$b\to a$	V 32040.42^h
$a^3\Pi$	x^k	1323.86^h	$9.20^{h,j}$	1.4135^h	0.0158^h	6.3^h	1.3083		
$(5p\pi)^1\Pi$	84217	(1675)		$(1.651_0)^l$		6.4^l	(1.210_6)	$(5p\pi)\gets X$	V 84217
$(5p\sigma)^1\Sigma^+$	83817.71	(1675)	8	(1.6275)		5.6	(1.2192)	$(5p\sigma)\gets X$	V 83817.71
$(5s\sigma)^1\Sigma^+$	82650.21			(1.557_8)		-21.3	(1.246_2)	$(5s\sigma)\gets X$	V 82650.21
$(4p\pi)^1\Pi$	80681.98	(1673)		1.651_6	0.0162	6.5	1.210_3	$(4p\pi)\gets X$	V 80681.98
$(4p\sigma)^1\Sigma^+$	79763.28	1666.6	12.7	1.6381	0.0174	6.4	1.2153	$(4p\sigma)\gets X$	V 79763.28
$(3d\sigma)^1\Sigma^+$	78691.21			(1.651_1)		13.0	(1.210_5)	$(3d\sigma)\gets X$	V 78691.21
$(3d\pi)^1\Pi$	77542.79			(1.672_3)		6.8^m	(1.202_8)	$(3d\pi)\gets X$ / $(3d\pi)\to A$	V { 77542.79 / 26454.1 }
$(4s\sigma)^1\Sigma^+$	77096.41	(1685.7)		1.605_4	0.0147	1.2^n	1.227_6	$(4s\sigma)\leftrightarrow X$ / $(4s\sigma)\to(3s\sigma)$	V { 77096.41 } / R { 11597.1^p }
$(3d\delta)^1\Delta$	76384.43			(1.6209)		6.4	(1.2217)	$(3d\delta)\to A$	V 25295.69
$(3p\pi)^1\Pi$	72286.05	(1673.0)	14^q	1.628_6	0.0169	6.3	1.218_9	$(3p\pi)\leftrightarrow X$	V 72286.06
$(3p\sigma)^1\Sigma^+$	69135.19	1613.2	14.5	1.6238	0.0194	7.3	1.2207	$(3p\sigma)\leftrightarrow X$ / $(3p\sigma)\to A$	V { 69135.19 / 18046.5^p }
$(3s\sigma)^1\Sigma^+$	65499.42	1692.9	12.4	1.6590	0.0178	7.6	1.2076	$(3s\sigma)\leftrightarrow X$ / $(3s\sigma)\to A$	V { 65499.42 / 14410.7^p }
$A^1\Pi$	51088.66	1264.96^r	$12.53^{r,s}$	1.4226	0.0180^t	7.3	1.3041	$A\leftrightarrow X$	R 51088.66
$X^1\Sigma^+$	0	1402.13^r	$11.84^{r,u}$	1.5174	0.0198^v	7.57	1.2626		
$B^{11}F^+$									
$X^2\Sigma^+$	89650^w	$(1680)^w$		1.64^w			1.21		

$D_0{}^0 = 7.81 \pm 0.13^a$ eV; IP $= 11.115 \pm 0.004$ eV

[a]Murad, Hildenbrand, and Main (1966).
[b]All quantities, except where noted, are in units of cm⁻¹.
[c]$(\omega_e) = \Delta G(\tfrac{1}{2})$.
[d]$(B_e) = B_0$.
[e]See Table VI for q values of $^{1,3}\Pi$, $^1\Delta$ states.
[f]$(r_e) = r_0$.
[g]$\gamma_e = 0.0002$.
[h]Barrow et al. (1958).
[i]$\gamma_e = -0.0012$.
[j]$\omega_e y_e = 0.047^h$.
[k]$A = 24.25$.
[l]Computed from Morse potential isotopic ratios and data for ¹⁰BF.
[m]$D_c = 10.9 \times 10^{-6}$.
[n]$D_1 = 22.8 \times 10^{-6}$.
[p]Robinson (1963).
[q]Chrétien (1950).
[r]Onaka (1957).
[s]$\omega_e y_e = -0.242^r$.
[t]$\gamma_e = -0.00040$.
[u]$\omega_e y_e = 0.056^r$.
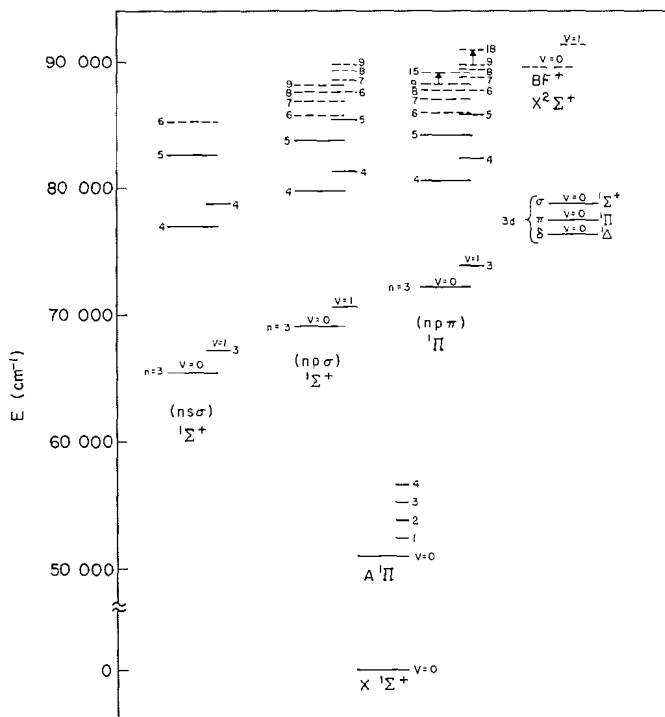[v]See Section $D(1)$.
[w]Computed from Rydberg series of BF.

FIG. 2. Term diagram for the singlet electronic states of ^{11}BF and ^{11}BF$^+$. States indicated by a solid line have been determined from band origins, those indicated by a dashed line from band heads.

constants given in Table III are more accurate than his values. The vibrational constants given by Onaka reproduce the band origins we have observed, within the experimental accuracy.

D(3) The (nsσ) Band Systems

We have observed a series of Σ–Σ band systems in absorption which we have assigned to the (nsσ)–X transitions. Rotational analyses of the bands associated with states having n values of 3, 4, and 5 have been carried out. The 0–0 band of the (6sσ)–X transition has been observed only on first-order spectra where the resolution is insufficient to permit a rotational analysis. These band systems decrease rapidly in intensity with increasing n values—states with n > 6 have not been observed.

The band heads of the (3sσ)–X band have previously been measured by Chrétien (1950) and by Mal'tsev (1960); the rotational constants of the excited state have been determined by Robinson (1963), who measured the (3sσ)–A emission bands. In the present work, we have measured the 0–0, 1–0, and 2–0 bands of the

absorption spectrum. The bands appear to be entirely free from local perturbations.

The (4sσ)–X band system has been observed in emission by Mal'tsev and the 0–0 band of the (4sσ)–(3sσ) transition has been measured by Robinson. In the present work, the rotational structures of the 0–0 and 1–0 bands of the absorption spectrum have been measured.

The 0–0 band of the (4sσ)–X system, shown in Fig. 4(a), is free from local perturbations but, in the 1–0 band, both the intensities and the positions of the lines of the R branch appear to be perturbed beyond R(16). Since the lines of the P branch beyond P(17) are lost in the head and the R branch is weak beyond R(16), we have not been able to determine the nature of the perturbation.

Only the 0–0 band of the (5sσ)–X system has been measured. This band shows one small perturbation in which the J = 13 level of the (5sσ) state is displaced downward by 0.85 cm^{-1}.

The rotational structure of the 0–0 band of the (6sσ)–X system was not measured since only first-order spectra were available. It appears, however, that the distance from the head to the

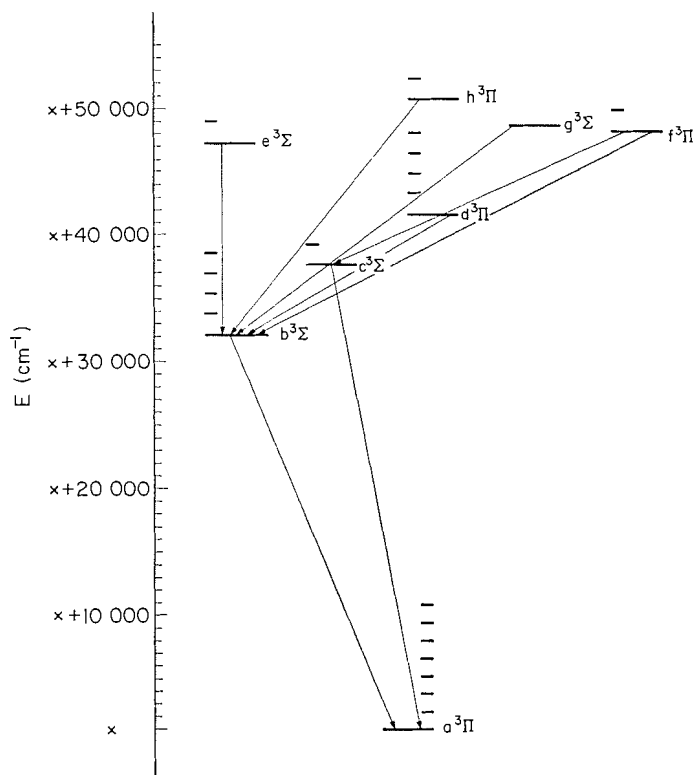FIG. 3.   Term diagram for the triplet electronic states of [11]BF.

origin of this band is somewhat greater than in the $(5s\sigma)-X$ bands, thus indicating that the B value of the excited state is somewhat smaller than that of the $(5s\sigma)$ state.

D(4)   The (npσ) Band Systems

The $(np\sigma)-X$ series of $\Sigma-\Sigma$ band systems is strong and is observed for n values from 3 to 9 inclusive. The rotational structures of the 0–0, 1–0, and 2–0 bands of the $(3p\sigma)-X$ and $(4p\sigma)-X$ systems and the 0–0 band of the $(5p\sigma)-X$ system have been analyzed. The $(3p\sigma)-X$ system had previously been observed in emission by Chrétien (1950) and by Mal'tsev (1960); Robinson (1963) has measured the $(3p\sigma)-A$ emission bands. No local perturbations have been observed.

For $n \geq 6$, where we are limited to first-order spectra, only band heads have been measured. The rotational structures of the transitions involving $n = 6$ and 7 appear, from the contours of the bands, to be similar to those of lower members of the series and one is led to the conclusion that the B values of the excited states change very little with increasing values of n. The

transitions are strong up to $n = 7$, but at $n = 8$ the intensity drops suddenly. For $n > 9$ this series merges with the $(np\pi)$ series and no bands with $n > 9$ are observed.

D(5)   The (npπ) Band Systems

The most intense series of Rydberg bands in the absorption spectrum of BF are $\Pi-\Sigma$ bands which have been assigned to the $(np\pi)$ series. The rotational structures of the 0–0 and the 1–0 bands of the $(3p\pi)-X$ and $(4p\pi)-X$ systems and the 0–0 band of the $(5p\pi)-X$ system have been analyzed. The 1–0 band of the $(3p\pi)-X$ system is shown in Fig. 4(b). The $(5p\pi)-X$ band which occurs near the short-wavelength limit of our high-order spectra was difficult to photograph and, since we obtained a much better plate of the [10]BF spectrum than of [11]BF, only the [10]BF spectrum was measured.

For values of n greater than 5 where high-order spectra were not available, only band heads have been measured. The members of this series with n values of 6, 7, and 8 are readily identified. It appears that the series of 0–0 bands can be
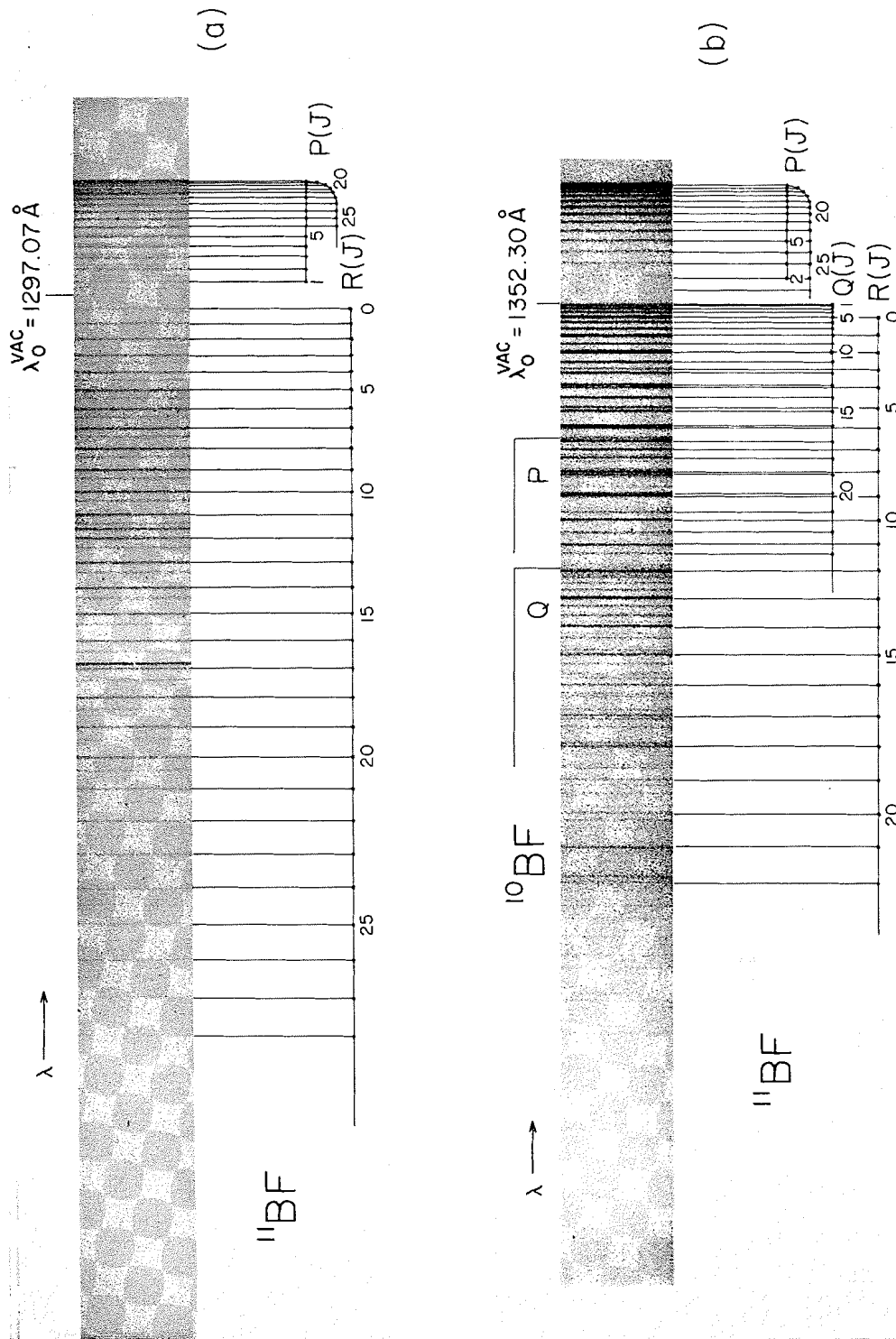
PLATE I

FIG. 4. (a) $(4s\sigma)^1\Sigma^+ - X^1\Sigma^+$ (0–0) band; (b) $(3p\pi)^1\Pi - X^1\Sigma^+$ (1–0) band.
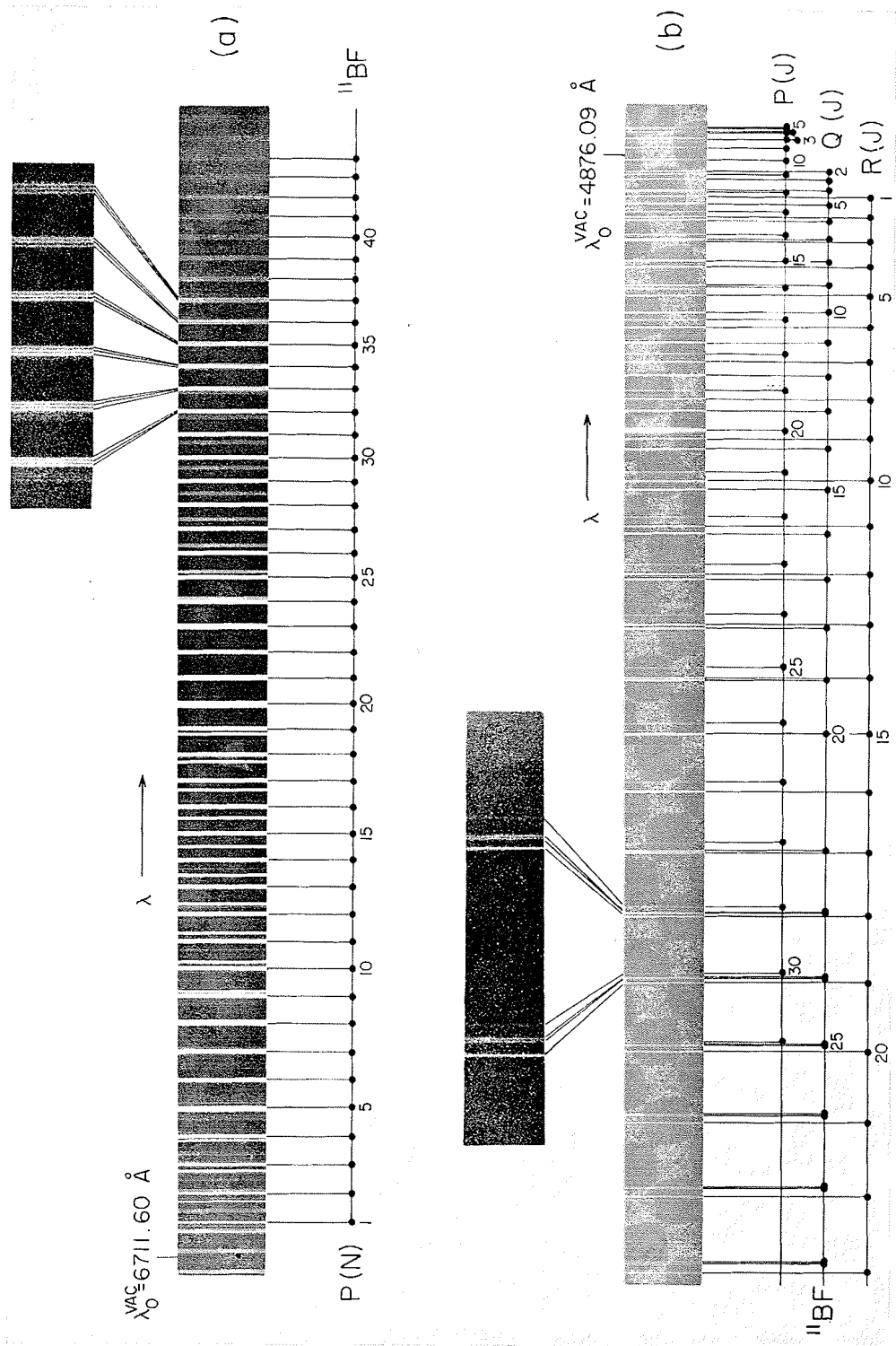
PLATE II

Fig. 5. (a) $e^3\Sigma^+ - b^3\Sigma^+$ (0–0) band: P branch; (b) $(3\textit{l}\delta)^1\Delta - A^1\Pi$ (0–4) band.

extended up to $n = 15$ and the series of 1–0 bands up to $n = 18$. The very high frequency portion of the spectrum is discussed in Section $D(7)$.

D(6) The (3dλ) Band Systems

A weak Σ–Σ band at 1270 Å has been assigned as the 0–0 band of the $(3d\sigma)$–X system. This band is somewhat overlapped by the 1–0 band of the $(4s\sigma)$–X system. The band shows no local perturbations.

A weak Π–Σ band which occurs at 1289 Å has been assigned to the $(3d\pi)$–X transition. This band shows no perturbations but does show an anomalous intensity distribution in the P, Q, and R branches. Unlike the corresponding branches in the $(np\pi)$–X bands, in these branches, no lines with J less than 6 can be observed and the R branch is very weak compared with the P and Q branches. The $(3d\pi)$ state also differs from the $(np\pi)$ states in that it shows a much larger Λ doubling and the effective D value, as determined from P and R branches, is anomalously high.

The $(3d\pi)$ state also appears in combination with the $A^1\Pi$ state in a weak system of emission bands beginning at 3870 Å and extending to longer wavelengths. These bands were observed, but not analyzed, by Robinson. The only band of this system which is sufficiently strong and free from overlapping to be suitable for measurement is the 0–1 band at 3966 Å. The band consists of two R branches and two somewhat stronger P branches, the doubling of the branches being caused by the Λ doubling. Both pairs of branches begin abruptly at $J = 7$; the lines beyond $P(22)$ and $R(10)$ are overlapped by the 0–0 band of the $(3d\delta)$–A system.

The $(3d\delta)$ state has been observed in a $(3d\delta)$–A transition. Robinson observed a band system in emission with band heads at 3954 and 4157 Å which he assigned to an $E^1\Sigma$–$A^1\Pi$ transition. We have observed five bands ($v' = 0$, $v'' = 0$, ..., 4) of this system at higher resolution and have measured the 0–0 and 0–4 bands. Our measurements, in agreement with Robinson, show that the lower state is the $A^1\Pi$ state. Our plates also show that, at high J values, the lines of the Q branch are resolved into doublets (see Fig. 5(b)) and that the first lines of the P, Q, and R branches have J values of 3, 2, and 1, respectively. This behavior leaves no doubt that the upper state is a $^1\Delta$ state. The fact that the Q branch, but not the P and R branches, is resolved into doublets is

readily understood. If the Λ doubling constants in the $^1\Delta$ and $^1\Pi$ states have the same sign, then the doublet separation in the Q branch lines will be the sum of the Λ splitting of the two states, while that in the P and R branches will be the difference. Thus, if the Λ doubling in the two states has nearly the same magnitude, the doubling of the P and R branches may remain unresolved while that in the Q branch is readily resolved. If we assume that the Λ doubling in the Δ state can be represented approximately by $q_\Delta J^2(J + 1)^2$ (see Table VI) then, from the observed separation of the doublets of the Q branch and the known Λ doubling of the $A^1\Pi$ state, we find the value of q_Δ of the Δ state to be -4×10^{-7} cm^{-1}.[4]

D(7) Rydberg States Near the Ionization Limit

In the 1100–1150 Å range, the absorption spectrum shows a large number of bands which can be arranged into two Rydberg series. The series at shorter wavelength is readily followed but, because of overlapping by members of the short-wavelength series and other bands, the long-wavelength series is difficult to pick out. In the spectrum of ^{10}BF, all members of the short-wavelength series show an isotope shift of about 50 cm^{-1} while the members of the other series show no appreciable shift. Since 50 cm^{-1} is the isotope shift characteristic of 1–0 bands of Rydberg transitions of BF, it is clear that the two series are the 1–0 and 0–0 bands of Rydberg transitions. This is further confirmed by the fact that the two nearly identical series are separated by about 1680 cm^{-1}, which agrees with the vibrational interval found in the lower Rydberg states. The two series are shown in Fig. 6.

Although the Rydberg series are readily followed near their short-wavelength limits and the lower members of the series have been analyzed in detail, it is not at once clear how to connect the low and high members of the series. The portion of the series which we have labelled $n = 8$, 9, and 10 in Fig. 6 is quite confusing since the intensities of these band heads appear to be less than those at either higher or lower n values.

---

[4]The Mulliken notation as modified by Herzberg (1950) has been used to describe the two series of rotational levels of opposite parity which are characteristic of each vibronic level of states having electronic orbital angular momentum. The rotational levels which behave like those of a $^1\Sigma^+$ state are called c levels and levels which behave like those of a $^1\Sigma^-$ state are called d levels. q is positive if the c levels lie above the d levels.

It is quite probable that the intensities of the band heads do not represent the true intensities of the bands. For low values of n, the band heads are far removed from the band origins and represent only a small fraction of the total band intensity but, for high values of n, it is probable that we are observing some type of a complex in which a large portion of the intensity is in the feature we have measured. The indefinite and changing nature of the feature we have measured reduces our accuracy. The most consistent interpretation of the series, based on an extrapolation of the $(np\sigma)$ and $(np\pi)$ series to a common limit is that the bands are due to $(np\pi)-X$ transitions. For n greater than 9, the $(np\pi)$ and $(np\sigma)$ states have essentially coalesced within the resolving power used here. It is probable that the two states interact to such an extent that it is no longer useful to designate them as separate states. Thus, although the measured features have been labelled $(np\pi)-X$ in Table II, it is probable that they are more complex than this notation indicates. The assignment of the series and the ionization potential is discussed further in Section E.

D(8) Triplet States

All triplet states have been observed in emission band systems. No singlet–triplet transitions have been observed and the relative energies of the singlet and triplet states is unknown. The $b^3\Sigma^+-a^3\Pi$ and $c^3\Sigma^+-a^3\Pi$ systems are very strong on our plates but we have not repeated or extended the work of BPWZ on these systems, except for a rough measurement of the 2–7 band of the $b-a$ system. We have, however, corrected and extended the analysis on other triplet states; this work is outlined in the following sections.

D(9) The $e^3\Sigma^+-b^3\Sigma^+$ System

These headless bands have recently been reported by Czarny and Felenbok (1968). In addition to the 0–0 band, we have been able to photograph and analyze the 1–1 band at 6679 Å (λ_0). The P branch of the 0–0 band is shown in Fig. 5(a).

As shown in the figure, the triplet splitting of the branches is clearly resolved but it is not sufficiently large to allow us to determine the splitting parameters for each of the states. A comparison of the lower-state B and D values with those found by BPWZ in the upper state of the $b^3\Sigma-a^3\Pi$ system leaves no doubt that the lower state of our transition is the $b^3\Sigma$ state. In all these conclusions, we are in agreement with Czarny and Felenbok.

D(10) The $f^3\Pi-b^3\Sigma^+$ and $f^3\Pi-c^3\Sigma^+$ Systems

Neither of these band systems has been reported previously. The Q head of the 0–0 band of the $f^3\Pi-b^3\Sigma$ system occurs at 9590 Å and the Q head of the 0–0 band of the $f^3\Pi-c^3\Sigma$ system at 6095 Å. The 0–0 band of both systems has been analyzed but only the lines of the Q branches of the 1–1 bands have been measured.

At first sight, these bands appear to be simple singlet–singlet bands (see Fig. 7(b)). Closer inspection reveals that the lines in all three branches are slightly broadened near the band origin and become progressively sharper as N increases. For N values greater than 4, all lines in the branches follow the formula expected for a $^1\Pi-^1\Sigma$ transition. If we assume that the widths of the lines at low N values is caused by the usual spin uncoupling of the $^3\Pi$ state, which is near case b coupling, then we find that the spin–orbit coupling constant of the $^3\Pi$ state is about 1 cm^{-1}.

The facts that the lower states of these band systems are the $b^3\Sigma$ and $c^3\Sigma$ states, and that they have a common upper state, are readily established. The combination differences of the upper states of the two 0–0 bands agree to within about 0.03 cm^{-1}. The lower-state constants agree with those determined by BPWZ for the $v = 0$ levels of the $b^3\Sigma$ and $c^3\Sigma$ states. Furthermore, the difference between the band origins of the $f^3\Pi-b^3\Sigma$ and $f^3\Pi-c^3\Sigma$ system is 5971.90 cm^{-1}, which may be compared with a value of 5971.55 cm^{-1} for the difference between the band origins of the $b^3\Sigma-a^3\Pi$ and $c^3\Sigma-a^3\Pi$ systems as determined by BPWZ. Considering that these values are the differences of four absolute wave number measurements, we believe that this agreement is satisfactory.

There is a rotational perturbation in the 0–0 band of the $f^3\Pi-c^3\Sigma$ system which can be traced to the fact that the three J levels for $N = 26$ in the $c^3\Sigma$ state are pushed downward by about 0.6 cm^{-1} without splitting the triplet degeneracy.

D(11) The $d^3\Pi-b^3\Sigma^+$ System

A strong sequence of bands occurs near 10 000 Å, with the strong Q branch head of the 0–0 band lying at 10 293.9 Å. These bands were observed by Robinson who assigned them as singlet transitions. We have measured and
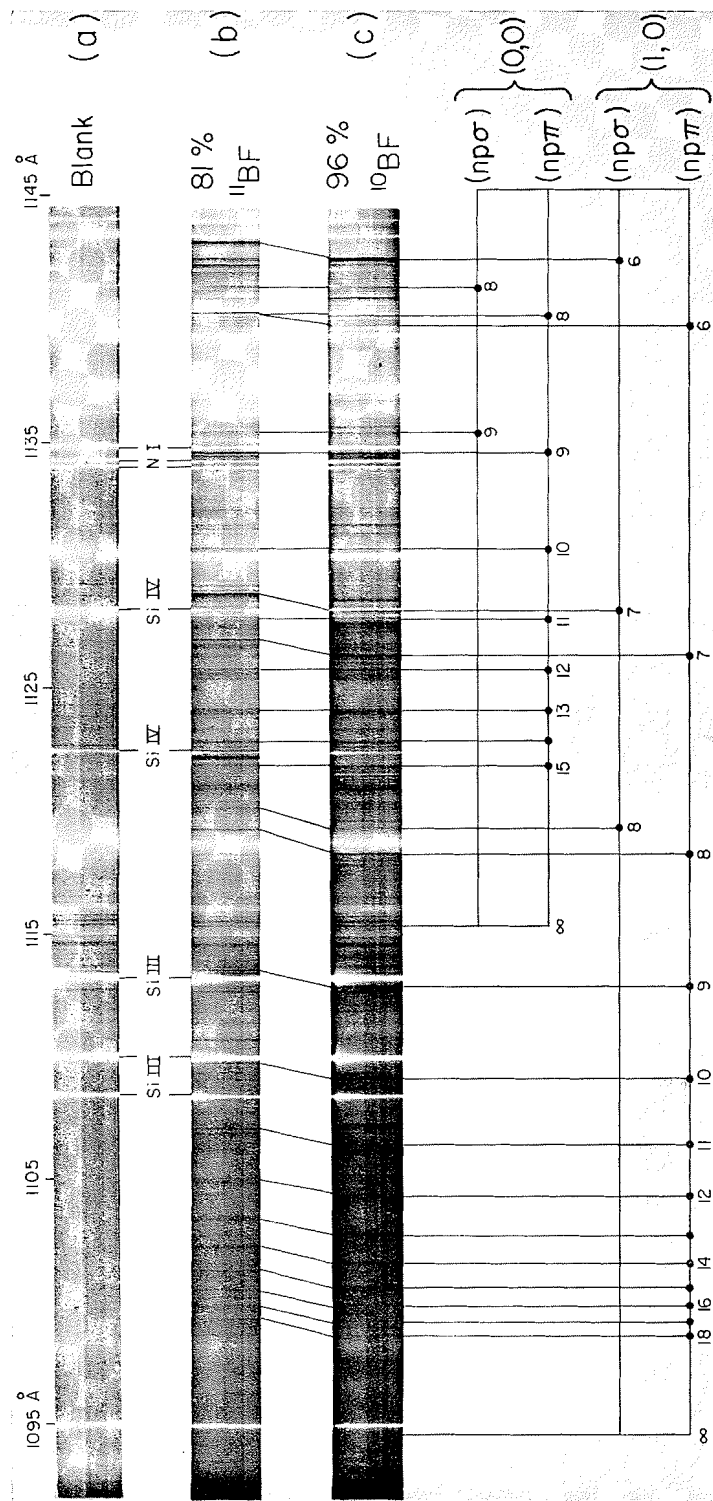
PLATE III

FIG. 6.   BF absorption spectrum near the first ionization limit.

PLATE IV

(a)

$\lambda \longrightarrow$

$\lambda_0^{VAC} = 10\ 296.91\ \text{Å}$

P (N)
Q(N)
R (N)

II BF

(b)

$\lambda \longrightarrow$

$\lambda_0^{VAC} = 9589.43\ \text{Å}$

P(N)
Q(N)
R (N)

II BF

FIG. 7. (a) $d\,^3\Pi - b\,^3\Sigma^+$ (0–0) band; (b) $f\,^3\Pi - c\,^3\Sigma^+$ (0–0) band.

analyzed the 0–0, 1–1, 2–2, 3–3, and 4–4 bands. The 0–0 band is shown in Fig. 7(a).

Unlike the two preceding $^3\Pi$–$^3\Sigma$ systems, there is no indication of triplet splitting in the bands of the 10 000 Å system. A photograph of the 0–0 band was taken with a 9 m Ebert spectrograph which would have readily detected a spin splitting as small as 0.01 cm^{-1}. No broadening of the lines was apparent, even in the $Q(1)$ and $P(2)$ lines.

In spite of the lack of triplet splitting in the observed lines, there is very strong evidence that the bands are due to triplet transitions. Combination differences for the lower state of the 0–0 band of this transition agree very well with those of the lower states of the 0–0 bands of the $f^3\Pi$–$b^3\Sigma$ and $e^3\Sigma$–$b^3\Sigma$ systems. The values of B_0'', B_1'', and B_2'' and the corresponding D values determined from the present measurements agree well with those reported by BPWZ for the $b^3\Sigma$ state, from measurements of the $b^3\Sigma$–$a^3\Pi$ bands. Also, neither the upper- nor the lower-state constants of the 10 000 Å bands agree with those of any observed singlet state, and the assignment of these bands to a singlet transition would require us to assume that they arise from two singlet states, neither of which had been observed in any of the previous experimental work.

The final proof that the lower state of this band system is the $b^3\Sigma$ state, comes from the observation of a perturbation in the 4–4 band. It is found that the $Q(26)$ line is displaced to higher frequencies by 0.6 cm^{-1} from its expected position. The constants of the b and c states show that the $N = 26$ level of the $v = 0$, $c^3\Sigma$ state lies at the same energy as the $N = 26$ level of the $v = 4$, $b^3\Sigma$ state. It has been pointed out in Section $D(10)$ that the $N = 26$ level of the $v = 0$, $c^3\Sigma$ state is displaced downward by 0.6 cm^{-1}. We must, therefore, conclude that, in the 4–4 band, we are observing the mutual perturbation between the $N = 26$ levels of the $v = 4$, $b^3\Sigma$ state and the $v = 0$, $c^3\Sigma$ state and that the lower state of the observed system is indeed the $b^3\Sigma$ state. Thus the experimental evidence that the 10 000 Å bands are triplets is overwhelming.

The 4–4 band consists of a Q branch only, thus indicating that one set of the Λ doublets of the $d^3\Pi$ state is predissociated. Such a predissociation can be caused by a $^3\Sigma^+$ state. Although the relative positions of singlet and triplet states are not known accurately, it appears that this predissoci-ation occurs at an energy considerably above the dissociation limit of the ground state and it therefore gives no information on the dissociation energy of BF.

D(12) The $g^3\Sigma$–$b^3\Sigma^+$ System

A weak headless Σ–Σ band has been observed with its band origin at 5906 Å. It is overlapped by the 0–1 band of the $(3p\sigma)$–A system. Lower-state combination differences show that the transition terminates on the $b^3\Sigma$ state. The triplet splitting causes the lines to become broad at high N values and the triplet components are resolved above $P(24)$. In this respect, the g–b band is similar to the e–b bands. There is a small perturbation in the $N = 12$ level of the upper state which causes the $R(11)$ and $P(13)$ lines to be split into two components of about equal intensity, separated by 0.12 cm^{-1}. The $P(19)$ line is also very broad relative to adjacent lines and it may also be somewhat perturbed. Unfortunately, the corresponding line of the R branch is overlapped and this perturbation cannot be confirmed.

D(13) The $h^3\Pi$–$b^3\Sigma^+$ System

The h–b system is overlapped by impurity emissions and by other BF bands but the Q head of the 0–0 band appears very clearly at 5200 Å. The band resembles the other $^3\Pi$–$^3\Sigma$ bands of BF and the lower-state combination differences from the rather weak P and R branches agree well with those of the $b^3\Sigma^+$ state. There are no local perturbations or other peculiarities in the 0–0 band. Only the Q head of the 1–1 band was measured. The first few lines of the branches seem to be broad and it appears that the h state has a triplet splitting similar to that of the f state.

D(14) The Spectrum of ^{10}BF

Although the ^{10}BF bands have not been listed and have been only occasionally mentioned in the previous sections, each band of ^{11}BF obtained from natural BF$_3$ is overlapped by one of ^{10}BF. The isotope shifts between corresponding bands of ^{10}BF and ^{11}BF unambiguously fix the vibrational assignments. For certain weak bands, such as those near the Rydberg series limit, spectra obtained from the BF$_3$ enriched in ^{10}B proved very valuable in assigning the bands. It was felt that little could be gained from analyzing the rotational structures of the ^{10}BF bands and this analysis has not been carried out.

E. Assignment of the Electronic States

*E(1) Electron Configurations and Ionization
Potential*

Although the analysis of the bands has presented few difficulties, the assignment of the observed electronic states to particular electron configurations has proved difficult. In the previous sections, the states have been designated by the symbols characterizing particular configurations, but no reasons have been given for these assignments. Here we shall consider the basis for the assignments.

The ground-state electron configuration of BF is

[a]　　　$KK(z\sigma)^2(y\sigma)^2(w\pi)^4(x\sigma)^2$　$X^1\Sigma^+$
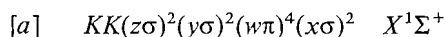
By analogy with CO, we should expect the first excited states to arise from the configuration:

[b]　　　$KK(z\sigma)^2(y\sigma)^2(w\pi)^4(x\sigma)(v\pi)$　$^1\Pi, {}^3\Pi$
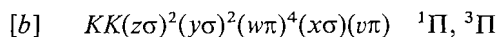
Since the $(v\pi)$ orbital is antibonding, these two Π states are expected to have B and ω values smaller than those of the ground state and, as in CO, the $^1\Pi$ state is expected to combine strongly with the ground state. The lowest observed excited singlet and triplet states of BF are those designated as the $A^1\Pi$ and $a^3\Pi$ states. The B and ω values of these two states are similar and are considerably smaller than the corresponding values for the ground state, and the $A^1\Pi–X^1\Sigma$ transition is strong. It appears certain that the $A^1\Pi$ and $a^3\Pi$ states can be assigned to the electron configuration [b].

If the behavior of BF is similar to that of CO, we might expect to observe states from other valence-electron configurations. These configurations involve either promoting an electron from the $(w\pi)$ to the $(v\pi)$ orbital or promoting an electron from either the $(w\pi)$ or $(x\sigma)$ orbital to the $(u\sigma)$ orbital. The states arising from these configurations should have B and ω values lower than those of the ground state. In fact, no states have been observed with these characteristics, other than the $A^1\Pi$ and $a^3\Pi$ states which have already been assigned and we must conclude that we have observed only one singlet and one triplet non-Rydberg excited state. This observation is in accord with the calculations of Nesbet (1965), who concluded that the two valence states from configuration [b] are the only valence states lying below the ionization limit.

The many Rydberg states can be represented by the configuration

[c]　　　$KK(z\sigma)^2(y\sigma)^2(w\pi)^4(x\sigma)$　$(nl\lambda)$
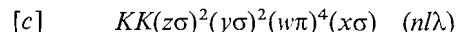
where n and l are the principal quantum number and the angular momentum quantum number of atom-like orbitals and λ is the quantum number representing the component of l along the molecular axis. The B and ω values for Rydberg states should be similar to those of the as yet unobserved BF^+ ground state. Although it is not clear whether these constants should be larger or smaller than those of the ground state of BF, the calculation of Nesbet (1965) indicates that they should be larger. We have observed a large number of states with B and ω values which are rather similar and which are larger than those of the ground state; we have concluded that these are Rydberg states.

Other Rydberg states could also be considered, for example, those arising from the configuration

[d]　　　$KK(z\sigma)^2(y\sigma)^2(w\pi)^3(x\sigma)^2(nl\lambda)$
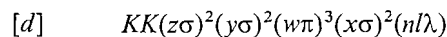
The B and ω values of these states would be expected to be similar to those of the first excited state of BF^+. By analogy with CO^+ and from the calculations of Nesbet (1965), we must conclude that the B and ω values of these states would be less than those of the ground state of BF. We have observed no such states and it is probable that these states lie beyond the first ionization limit.

Even with the evidence that all the observed Rydberg states belonged to series associated with the ground state of the ion, it was not clear how they should be assigned. Some of the difficulties in this respect have been discussed in the earlier work of Lefebvre-Brion and Moser (1965a) and Robinson (1963). Rydberg states, particularly those of high n and l values, might be expected to lie in groups, each associated with a particular value of n and l. Such l complexes have been observed for a number of molecules but perhaps those in BF might be expected to be similar to the well-studied complexes of NO. In BF, no recognizable complexes were found and we must conclude that the deviation from spherical symmetry of the core is so great that the separation of states of various λ values for a given n and l value is large and comparable to the separation of states of different n and l values. This implies that the assignment of a definite n, l, and λ value to an observed state is not strictly possible.

TABLE V

Observed Rydberg series and quantum defects of ^{11}BF

n	$(ns\sigma)$ (0–0) T_0	δ	(1–0) T_0	δ	$(np\sigma)$ (0–0) T_0	δ	(1–0) T_0	δ	$(np\pi)$ (0–0) T_0	δ	(1–0) T_0	δ
3	65499.4	0.868	67167.5	0.869	69135.2	0.687	70719.3	0.693	72286.0	0.486	73948.0	0.489
4	77096.4	1.045	78782.1	1.043	79763.3	0.669	81404.4	0.675	80682.0	0.502	82355.0	0.507
5	82650.3	1.041			83817.7	0.662	85477.1	0.670	84217	0.506	85892	0.516
6	85200	1.034			85805.8	0.658	87486	0.657	86018	0.503	87678	0.518
7					86922	0.658	88593	0.668	87038	0.518	88735	0.497
8					87614	0.658	89287	0.671	87678	0.540	89338	0.578
9					88074	0.654	89754	0.656	88121	0.528	89802	0.526
10									88427	0.528	90100	0.555
11									88648	0.535	90330	0.524
12									88815	0.536	90497	0.522
13									88946	0.515	90625	0.524
14									89046	0.521	90728	0.499
15									89129	0.487	90808	0.501
16											90874	0.487
17											90926	0.519
18											90974	0.443
	$(nd\sigma)$ (0–0)				$(nd\pi)$ (0–0)				$(nd\delta)$ (0–0)			
3	78691.3	−0.164			77542.8	−0.011			76384.3	0.124		
∞	89650		91330		89650		91330		89650		91330	

Whereas in l complexes, the rotation of the molecule mixes the various λ values for a given n and l, in BF it is probable that for a given λ the electronic wave functions of states of different n and l are mixed. Thus the rotational structure of the individual states is simple but the assignment of electron configurations is difficult. In spite of these difficulties, in each observed state it is likely that one particular set of $(nl\lambda)$ values predominate and we have attempted to identify this set and use it as a label for the state.

Another of the major difficulties in assigning the Rydberg states has been the lack of an accurate value for the ionization potential, and it was for this reason that we investigated the spectral region near the expected ionization limit. As discussed in Section $D(7)$ and illustrated in Fig. 6, we did observe series of 1-0 and 0-0 bands converging towards limits. In order to determine these series limits, it was necessary to determine the principal quantum numbers of the observed states and to fit the series to a suitable formula.

The electronic energies of Rydberg states are usually represented by

$$[1] \qquad T_{nl\lambda} = T_\infty - \frac{R}{(n^*)^2} = T - \frac{R}{(n - \delta_{l\lambda})^2}$$

where $T_{nl\lambda}$ is the term value, T_∞ is the ionization potential, R is the Rydberg constant, and n is the principal quantum number. $\delta_{l\lambda}$ is, to a first approximation, a constant but, to a higher approximation, varies slowly along the series. In the commonly accepted Rydberg–Ritz formula, δ varies according to the expression

$$[2] \qquad \delta_{l\lambda} = \alpha_{l\lambda} - \beta_{l\lambda}(n^*)^{-2}$$

and $\delta_{l\lambda}$ is commonly plotted against $(n^*)^{-2}$ to determine α and β. The values of $\delta_{l\lambda}$ to be expected are ~ 1 for $l = 0$, ~ 0.7 for $l = 1$, and ~ 0.1 for $l = 2$. For a given value of l the various states of different λ will have different values of $\delta_{l\lambda}$ and the spread of these values will depend in some complex manner on the deviations from spherical symmetry of the core.

It was found that the high members of the 0-0 and 1-0 series could be fitted, within the experimental accuracy, with the values $\delta = 0.52$, $T_\infty = 89\,650$ and $91\,330\,\text{cm}^{-1}$. It is not possible to change the series limits by more than a few cm^{-1} without reducing the accuracy of the fit. Assuming these values of T_∞, equation [1] has

then been used to calculate the quantum defect of each state; these values of δ are listed in Table V. In Fig. 8, the quantum defects are shown plotted against $(n^*)^{-2}$ for the $v = 0$ levels of the $(np\pi)$, $(np\sigma)$, and $(ns\sigma)$ series, and straight lines drawn through the observed points. If the ionization limit is changed by $5\,\text{cm}^{-1}$, the quantum defects of the $(p\sigma)$ states would follow the points marked $\times$ in the figure. Thus a consistent set of constants can be achieved in which the ionization limit is determined to within $\pm 5\,\text{cm}^{-1}$ and (except for the $(3s\sigma)$ state) the quantum defects vary slowly with $(n^*)^{-2}$.

Although the series limit, which fits the measurements, is determined to within $\pm 5\,\text{cm}^{-1}$, the ionization potential is not determined to this accuracy. As was pointed out in Section $D(7)$, we do not know the relationship between the features we have measured in the high members of the $(np\pi)$ series and the band origins. The P and Q heads of typical Rydberg bands may be separated by as much as $25\,\text{cm}^{-1}$ and it is possible that the features we have measured are P heads (or more likely neither P nor Q heads but some intensity maximum). For this reason we consider the
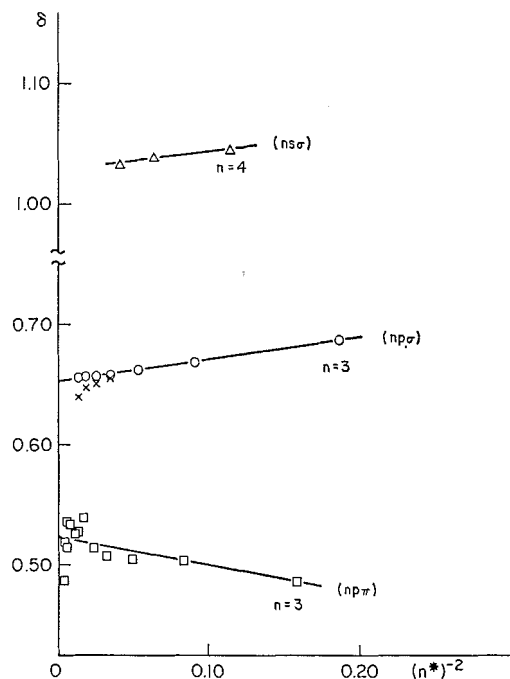

FIG. 8. Edlén plot for the $v = 0$ levels of the Rydberg series of BF with IP $= 89\,650\,\text{cm}^{-1}$. Points marked $\times$ were obtained with IP $= 89\,645\,\text{cm}^{-1}$.

TABLE VI

Observed and calculated Λ doubling in Π and Δ states

State	q^a	Perturbing state	q_{calc}^b $(l=1)$	q_{calc}^b $(l=2)$	$l(l+1)_{eff}$
$(3p\pi)^1\Pi$	0.0009	$(3p\sigma)$	0.0033		0.545
$(4p\pi)^1\Pi$	0.0056	$(4p\sigma)$	0.0144		0.982
$(5p\pi)^1\Pi$	0.0137	$(5p\sigma)$	0.0263		1.042
$(3d\pi)^1\Pi$	0.0423	$(4s\sigma)$	.	0.0708	3.584
		$(3d\sigma)$		−0.0284	
$(3d\delta)^1\Delta$	-4×10^{-7c}	$(3d\pi)(3d\sigma)$		-1×10^{-7}	
		$(3d\pi)(4s\sigma)$		-2×10^{-6}	
$d^3\Pi$	0.0011	$c^3\Sigma$	0.0018		1.222
$h^3\Pi$	0.0024	?			
$f^3\Pi$	−0.0289	$g^3\Sigma$		−0.0627	
		$e^3\Sigma$		0.0218	

$^a q = B(RP) - B(Q) = B_c - B_d$.

^{b}Assuming pure precession, $q_\pi = 2B^2 l(l+1)/(T_\pi - T_\Sigma)$.

^{c}Assuming Λ doubling follows $\Delta v = q_\Delta (J-1)J(J+1)(J+2) \approx q_\Delta J^2(J+1)^2$ and with pure precession, $q_\Delta = 2B^4(l-1)l(l+1)(l+2)/(T_\Delta - T_\pi)^2(T_\Delta - T_\Sigma)$.

ionization potential of BF to lie between 89 680 and 89 635 cm^{-1}, but we cannot specify it more closely.

If the band origins are assumed to lie 20 cm^{-1} higher in frequency than the observed features, then the true series limit will be increased by 20 cm^{-1}. In this case the linear relationship between δ and $(n^*)^{-2}$ disappears for small values of n in the $(np\sigma)$ series and the δ values for $(np\pi)$ series show a somewhat less regular variation with n. These considerations do not, however, give convincing evidence for the 89 650 cm^{-1} value of the ionization potential since there is no theoretical reason for believing that the quantum defects of the $(np\sigma)$ states of a molecule such as BF should follow the simple formula $\delta_{l\lambda} = \alpha_{l\lambda} - \beta_{l\lambda}(n^*)^{-2}$ and since the irregularity in the $(np\pi)$ series may arise from perturbations or from the variation from band to band of the feature we have measured.

Although there is still a considerable experimental error in determining the ionization potential, the smooth variation of δ with $(n^*)^{-2}$ for the various series shown in Fig. 8 does give us confidence that the band systems have been arranged into series correctly. It is not possible, for example, to interchange band systems between the $(ns\sigma)$ and $(np\sigma)$ series without seriously disturbing the regularity of the series. The most difficult problem is to determine whether or not the states we have assigned as $(4s\sigma)$ and $(3d\sigma)$ should be interchanged, and those assigned as $(5s\sigma)$ and $(6s\sigma)$ should be assigned as $(4d\sigma)$ and $(5d\sigma)$. In making our assignments, we have

depended largely on the intensities of the bands. An interchange of assignments would require that the $(3s\sigma)-X$ transition be very strong, and that the $(4s\sigma)-X$ and $(5s\sigma)-X$ transitions be much weaker and about equal in intensity. The assignment we have used gives a smoother decrease in intensity along the (ns) series. The $(np\pi)$ states are clearly identified as Π states by the structure of the bands and the higher members of the series join smoothly onto the lower members. The largest irregularity in the $(np\pi)$ series occurs at $n = 8$ in the series of 0–0 bands which falls at the same energy as the $n = 6$ member of the 1–0 series. Whether there is an interaction between these states or whether this is simply a matter of overlapping bands is not known, since the resolution is insufficient to analyze this complex region of the spectrum.

E(2) Λ Doubling of the Π and Δ States

If the Rydberg states can be represented by the $(nl\lambda)$ symbols described in Section $E(1)$, then it is to be expected that the Λ doubling of the Π states will be given by the pure-precession formula of Van Vleck in which

$$[3] \qquad q = \frac{2B^2 l(l+1)}{T_\Pi - T_\Sigma}$$

In this expression, T_Π and T_Σ are the term values of the Π and Σ states arising from an excited electron of given l value, q is the usual Λ doubling constant (Herzberg 1950), and B is the usual rotational constant. This expression is valid if $T_\Pi - T_\Sigma \gg 2BJ$. We have assigned observed Π

and Σ states as those corresponding to members of the (np) series for n values of 3, 4, and 5 and thus, for these Π states, q can be calculated.

The $(3p\pi)$, $(4p\pi)$, and $(5p\pi)$ states each exhibit Λ-type doubling which appears to be caused primarily by a lower-lying $^1\Sigma^+$ state; that is, B_c is greater than B_d. The observed values of the Λ doubling constant are given in the second column of Table VI and the values calculated from [3] are given in the fourth column. The agreement between the observed and calculated values is poor. The interaction between the $(4p\sigma)$ and $(4p\pi)$ states has been calculated exactly, assuming only that l is equal to unity (Bauer, Herzberg, and Johns 1964), and calculated energy levels compared with the observed levels in Fig. 9. We believe that the lack of agreement between the observed and calculated values is a clear indication that states of various (nl) values are mixed.

The effective l of a state is therefore not integral and the Λ doubling of each Π state results from a number of interactions.

The three states which have been assigned as $(3d\sigma)$, $(3d\pi)$, and $(3d\delta)$ show several peculiarities. The $(3d\delta)$ state is relatively well behaved but, as mentioned in Section $D(6)$, it does show a significant Λ-type doubling. The $(3d\pi)$ state shows several anomalies, the most significant of which are: (1) all lines of low J in the $(3d\pi)$–X and $(3d\pi)$–A bands are missing, (2) in the $(3d\pi)$–X band, the P and Q branches are much stronger than the R branch, (3) in the $(3d\pi)$–A band, the two P branches are somewhat stronger than the R branches, (4) the B and D values of the c component (corresponding to the P and R branches of the $(3d\pi)$–X band) are unusually large. The $(3d\sigma)$ band is unusual only in that the apparent D value is about twice as great as the D values of most other Rydberg states.

In addition to the anomalies mentioned in the previous paragraph, which are apparent from the analysis of the individual bands, a study of the relative energies of the observed states and their constants shows other anomalies. The state assigned as $(3d\sigma)$ lies above $(3d\pi)$ which in turn is above $(3d\delta)$. This ordering of the levels is inverted compared with that which is expected and which has been observed in other molecules by Jungen and Miescher (1969) and by Bauer, Herzberg, and Johns (1964). Furthermore, the Λ doubling in the $(3d\pi)$ state is of such a sign that it must arise from a Σ^+ state which lies lower and cannot be caused by the observed $(3d\sigma)$ state.

It appears certain that at least some of the anomalies in the $(3d\lambda)$ states arise from an interaction with the $(4s\sigma)$ state. The $v = 0$ level of the $(4s\sigma)$ state lies only 446 cm^{-1} below the corresponding level of the $(3d\pi)$ state and it is found to have anomalously low B and D values. The possibility that the anomalies in the $(3d\lambda)$ states could be explained by interchanging the assignments of the $(3d\sigma)$ and $(4s\sigma)$ states has been considered. However, as shown in Table VI, even with this change in assignment, the calculated value of q of the $(3d\pi)$ state is in error by a factor of two. It appears probable that the $(3d\sigma)$ and $(4s\sigma)$ states are mixed rather strongly and that the Λ doubling of the $(3d\pi)$ state results largely from some combination of the two states, each of which contains some d and some s character, and an interchange of the two states does not invalidate

FIG. 9. The $(4p)$ complex of ^{11}BF. The solid lines are theoretical curves for $l = 1$, calculated according to equation [3] of Bauer, Herzberg, and Johns (1964) using $T_0 = 79\ 759.86$, $A = 922.18$, and $B = 1.6396$ cm^{-1}. The circles indicate the observed energies of the Σ^+ and Π^+ levels and the crosses indicate the Π^- levels. The quantity $BJ(J + 1)$ has been subtracted from the energy.

this conclusion. Even this explanation, involving the mixing of the $(4s\sigma)$ and $(3d\sigma)$ states, is too simple since, as has been pointed out above, the interaction of the $(p\sigma)$ and $(p\pi)$ states does not follow the pure-precession rule and it is probable that there is a mixing of the p states with s and d states.

We have not been able to determine the cause of the peculiar intensity distribution in the $(3d\pi)$–X band. The relative intensities of the P and R branches in a Π–Σ transition can be influenced by the interaction of the Π state with another Σ state (MacDonald 1932; Huber 1964). If we assume that the $(3d\pi)$ state interacts weakly with a Σ state which is connected to the ground state by a strong transition moment, then this mechanism could explain the observed ratio of P, Q, and R branch intensities. This mechanism will not, however, explain the very low intensity of the lines of low J values in all three branches in both the $(3d\pi)$–X and $(3d\pi)$–A bands. We are tempted to invoke some predissociation of the c$^-$ type described by Mulliken (1960), but the evidence to support this is very limited.

Also, the slight difference in the intensities in the P and R branches of the $(3d\pi)$–A transition remains unexplained but here the effect is a small one and even the experimental evidence for its existence is somewhat suspect.

E(3) Triplet States

All data on the triplet states have come from emission spectra and are much more limited than the data on the singlets. Unsuccessful attempts were made to observe absorption to the triplet Rydberg states from the lowest triplet state with the flash discharge apparatus. We have found no connection between the singlet and triplet manifold and the triplet Rydberg states cannot be followed to sufficiently high n values for an accurate determination of their energies with respect to the ionization limit.

The lowest triplet state which has been observed is the $a^3\Pi$ state. The constants of this state have been determined by BPWZ and we have made no further measurements. The vibrational and rotational constants of this state are similar to those of the $A^1\Pi$ state and, as will be discussed later, it lies considerably below the A state. There can be no doubt that the $a^3\Pi$ state is the valence state corresponding to electron configuration $[b]$. All other triplet states have constants similar

TABLE VII
Rydberg assignments of triplet states

Present designation	Rydberg designation	Singlet–triplet separation[a] (cm^{-1})
$b^3\Sigma^+$	$(3s\sigma)$	4843
$c^3\Sigma^+$	$(3p\sigma)$	2507
$d^3\Pi$	$(3p\pi)$	1918
$e^3\Sigma^+$	$(4s\sigma)$	1540
$f^3\Pi$	$(3d\pi)$	486
$g^3\Sigma^+$	$(3d\sigma)$	1107
$h^3\Pi$	$(4p\pi)$	800

[a]See Section $E(3)$.

to those of the singlet Rydberg states and, by arguments similar to those used for the singlet states, we conclude that these triplets are Rydberg states.

The proposed assignments for the triplet Rydberg states are given in Table VII. The assignment of the $b^3\Sigma$, $c^3\Sigma$, and $d^3\Pi$ states as $(3s\sigma)$, $(3p\sigma)$, and $(3p\pi)$ follows from the similarity to the corresponding singlet states of their relative energies and other characteristics. The separation of the singlet and triplet states of the same electron configuration are expected to decrease rapidly with increasing n and, for a molecule as light as BF, the separation is expected to be small even for $n = 3$. Thus the triplet-state term values might be expected to follow the same pattern as the singlet term values being slightly depressed at low n values. Once having assigned the $(3s\sigma)$, $(3p\sigma)$, and $(3p\pi)$ states, it might be expected that the remaining triplet states could be assigned unambiguously by comparison with the singlet states. No such simple correlation exists and the assignment is made more difficult by the fact that some relatively low-lying Rydberg states have escaped detection. In Table VII, the three observed Π states have been assigned to $(3p\pi)$, $(3d\pi)$, and $(4p\pi)$. The $(4p\pi)$ singlet and triplet states have arbitrarily been given a separation of 800 cm^{-1} in column 3 of the table and the two upper $^3\Sigma$ states have then been assigned to give singlet–triplet separations which appear most reasonable. With these assignments, it is clear that the $(4p\sigma)$ and $(3d\delta)$ triplet states should lie in the energy range covered by the table but these two states have not been found.

Although the value of 800 cm^{-1} for the singlet–triplet separation is arbitrary, it is the value given by Lefebvre-Brion and Moser (1965a) and, from a comparison with the values for other

atoms and molecules, we believe it is unlikely to be in error by more than ± 1000 cm^{-1}. From this it follows that the $a^3\Pi$ state should lie at 28 616 $\pm$ 1000 cm^{-1}. We have attempted to find the $a^3\Pi-X^1\Sigma$ band system but have found no absorption in the 3000–4000 Å region under conditions where BF absorption is very strong. This is to be expected in view of the path lengths and pressures necessary to observe the analogous transition in CO. The emission spectrum in this region is dominated by the very strong $b–a$ and $c–a$ systems, and we have not investigated rather special sources which might favor the triplet–singlet emission.

The Λ doubling and the triplet splitting of an electronic state often yield information useful in assigning the electron configuration of the state but, in the triplet states of BF, they have proved to be of little value. In Table VI, observed values of the Λ doublings of the $^3\Pi$ states are given and are compared with values calculated on a pure-precession model. As with the singlet states, the agreement between the observed and calculated values is poor. The triplet splitting of all Rydberg states is very small and we have been unable to determine the spin-splitting constants for any of the states. Only in the valence state, $a^3\Pi$, do we find an appreciable spin splitting and, for this state, $A = 24$ cm^{-1} which is similar in magnitude to the values found in the corresponding states of N$_2$ (42.3 cm^{-1}), CO (41.3 cm^{-1}), and AlF (46 cm^{-1}).

F. General Discussion

In Sections $E(1)$ and $E(2)$, it has been stated that the various Rydberg states of BF interact so strongly that it is difficult to assign them simple one-electron configurations. It is useful to review the evidence for this mixing.

Each of the Rydberg states interacts not only with other Rydberg states but also in some specific way with valence states. Since the energies of the singlet and triplet valence states of BF are quite different, these interactions probably account for the fact that the singlet and triplet Rydberg states do not have the same relative energies. The $(3d\sigma)–(3d\pi)$ separation, for example, is much smaller for the triplet than the singlet states. Since the valence states of BF are far removed from the Rydberg states, the valence–Rydberg interaction should have rather little effect on the l value of the Rydberg states, as

determined by [3]. The Λ-type doubling constants in Table VI show that the effective l values of the states are far from integral values. These effective l values are in themselves meaningless but they do indicate that two-state interactions, with an integral l value, do not give even approximately the correct q values. It is clear that interactions between Rydberg states of different n and l are necessary to account for the observed q values.

The observed B and D values also show strong evidence of interactions between states. All Rydberg states should have very similar B values and perhaps only the lowest, $(3s\sigma)$, should show an appreciable deviation from the B value of the ion. The B values we have found vary from 1.557 to 1.672 cm^{-1}. It is clear that the variation results from interaction between states but it is not possible to eliminate the effects of these interactions by averaging over the λ states of a given n and l value. We have, therefore, concluded that there are complex interactions between the Rydberg states and it is interesting to note that the interactions are such that the observed spectrum remains remarkably simple.

A number of interesting comparisons which can be made between the observed and calculated constants of the three isoelectronic molecules N$_2$, CO, and BF are presented in Table VIII. As has been noted by Nesbet (1964), there is a marked improvement in the calculated values as we go from N$_2$ to BF. The calculated ionization potential of BF and the vibrational frequency and B_e value of BF$^+$ are very close to the observed values found in this work. One interesting set of experimental values is the set of $(3p\pi)^1\Pi–(3p\sigma)^1\Sigma$ separations where the large value for BF is compared with the much smaller value for CO and the still smaller value for N$_2$. The tendency of the spectrum to show "l-complexes" depends upon this separation; the values in the table show the reason for the lack of complexes and the relative simplicity of the BF spectrum.

Lefebvre-Brion and Moser (1965a) have carried out calculations on the Rydberg states of BF. Their suggestion, that certain states assigned as singlets by Robinson (1963) are indeed triplets, has been confirmed in our experimental work. A meaningful comparison of observed and calculated values is difficult for Rydberg states. Given the ionization potential, the term values of the Rydberg states, particularly the higher states, can be determined within a fraction of an electron volt

TABLE VIII

A comparison of some observed and calculated constants of N_2, CO, and BF

	N_2		CO		BF	
	Obs.	Calc.	Obs.	Calc.	Obs.	Calc.
$\omega_e(X^1\Sigma^+)$	2358.1[a]	2722.4[i] 2729.6[j]	2169.8[m]	2357.2[i] 2431[s]	1402.1[v]	1413.8[i] 1496[s]
$B_e(X^1\Sigma^+)$	1.9987[a]	2.094[i] 2.121[j]	1.9313[m]	1.965[i] 2.027[s]	1.5165[w]	1.495[i] 1.559[s]
$\omega_e\left(\dfrac{AB^+}{X^2\Sigma^+}\right)$	2207.2[a]	2460.5[k] 2570.5[j] 2300[l]	2214.2[m]	2331.8[k]	~1700[x]	1662.5[k]
$B_e\left(\dfrac{AB^+}{X^2\Sigma^+}\right)$	1.932[a]	1.997[k] 2.065[j]	1.977[m]	2.015[k]	~1.64[x]	1.621[k]
$T_0(A^1\Pi)$	68951[a,b]	81580[k]	64747[m]	75800[k]	51089[v]	57500[k]
$T_0(a^3\Pi)$	59310[a,c]	65908[k]	48474[m]	48700[k] 46500[t]	(28600)[x,z]	25174[k]
IP(eV)	15.580[a]	17.368[k] 16.01[j]	14.016[m]	15.423[k] 14.978[s]	11.115[x]	11.194[k] 10.928[s]
$(3p\pi)^1\Pi$ $-(3p\sigma)^1\Sigma^+$	<100[d,e]	—	1011[m,n]	~0[u]	3151[x]	2178[y]
$(3s\sigma)^1\Sigma^+$ $-(3s\sigma)^3\Sigma^+$	~3250[f,g]	4839[l]	3084[m,p]	5646[u]	(4843)[x,z]	6372[y]
$(3p\sigma)^1\Sigma^+$ $-(3p\sigma)^3\Sigma^+$	800[e,h]	800[l]	913[o]	800[u]	(2507)[x,z]	1613[y]
$(3p\pi)^1\Pi$ $-(3p\pi)^3\Pi$	?	800[l]	853.2[q,r]	800[u]	(1918)[x,z]	2339[y]

NOTE: All quantities in units of cm⁻¹, unless otherwise noted. The number of figures quoted often exceeds the accuracy claimed for the calculation.
[a]Lofthus (1960).
[b]$a^1\Pi_g$.
[c]$B^3\Pi_g$.
[d]Term difference between $c^1\Pi_u$ and $c'^1\Sigma_u{}^+$.
[e]Dressler (1969).
[f]$a''^1\Sigma_g{}^+$ and $E^3\Sigma_g{}^+$.
[g]Lutz (1969).
[h]$c'^1\Sigma_u{}^+$ and $D^3\Sigma_u{}^+$.
[i]Nesbet (1964).
[j]Cade, Sales, and Wahl (1966).
[k]Nesbet (1965).
[l]Lefebvre-Brion and Moser (1965b).
[m]Krupenie (1966).
[n]$E^1\Pi$ and $c^1\Sigma^+$.
[o]Tilford and Vanderslice (1968).
[p]$B^1\Sigma^+$ and $b^3\Sigma^+$.
[q]$E^1\Pi$ and $c^3\Pi$.
[r]Tilford (1969).
[s]Huo (1965).
[t]Huo (1966).
[u]Lefebvre-Brion, Moser, and Nesbet (1964).
[v]Onaka (1957).
[w]Calder and Ruedenberg (1968).
[x]Present work.
[y]Lefebvre-Brion and Moser (1965a).
[z]Numbers in ( ) depend upon the procedure outlined in Table VII and Section E(3).

from typical values of quantum defects which are well known from atomic and molecular spectra. Thus, for the assignment of states, more advanced calculations are required only if we are required to differentiate between states of the same symmetry which are very closely spaced or if, with insufficient experimental data, we are forced to assign states by means of small effects such as the Λ doubling or the small energy differences between states of an *l* complex. Although the energies calculated by Lefebvre-Brion and Moser (1965) (corrected for the new value of the ioniza-

tion potential by adding 0.18 eV) agree quite well with the observed values,[5] the calculations cannot yet predict these finer details accurately. For example, the calculated difference between $3p\sigma$ and $3p\pi$ is 0.27 eV and the observed value 0.39 eV. It is interesting to note that the calculations

[5]We wish to thank Dr. Lefebvre-Brion for pointing out to us that there are some errors in columns 4 and 5 of Table VII of her paper (Lefebvre-Brion and Moser 1965a). A $^1\Sigma^+$ ($4p\sigma$) state should be added at 9.78 eV; the 10.28 eV state should be assigned to ($4d\sigma$); and the 10.68 eV state and its assignment should be deleted.

　　　CANADIAN JOURNAL OF PHYSICS. VOL. 48, 1970

place the ($4s\sigma$) state above the ($3d\sigma$) whereas, as discussed in Section $E(1)$, with rather little experimental evidence, we have assigned the higher state to the $3d\sigma$ configuration and here the calculations may well be correct.

In spite of the large number of band systems which have been observed, much remains unknown. The complex region of the absorption spectrum involving the $n = 7$, 8, and 9 states probably could be analyzed if high-order spectra could be obtained but, with our present apparatus, we cannot obtain these spectra. The triplet states have been only rather poorly defined in the present work and it is not clear how additional states could be found. We have found no triplet–singlet transitions but it is possible that, with certain types of sources, the $a^3\Pi–X^1\Sigma$ system can be observed in emission. We searched for the emission spectrum of BF^+ and failed to find it but future experiments may be successful. Our work has yielded no information on the dissociation energy of BF and it appears unlikely that the spectrum will be useful in determining this quantity. Finally, since we have observed BF to have a long lifetime, it appears probable that the microwave spectrum can be observed and, from this spectrum, it should be possible to obtain hyperfine-structure constants and the dipole moment of the ground state.

BARROW, R. F., PREMASWARUP, D., WINTERNITZ, J., and ZEEMAN, P. B. 1958. Proc. Phys. Soc. (London), A, 71, 61.
BAUER, S. H., HERZBERG, G., and JOHNS, J. W. C. 1964. J. Mol. Spectry. 13, 256.
CADE, P. E., SALES, K. D., and WAHL, A. C. 1966. J. Chem. Phys. 44, 1973.
CALDER, G. V. and RUEDENBERG, K. 1968. J. Chem. Phys. 49, 5399.
CHRÉTIEN, M. 1950. Helv. Phys. Acta, 23, 259.
CZARNY, J. and FELENBOK, P. 1968. Chem. Phys. Lett. 2, 533.
DOUGLAS, A. E. and POTTER, J. G. 1962. Appl. Opt. 1, 727.
DRESSLER, K. 1969. Can. J. Phys. 47, 547.
HERZBERG, G. 1950. Spectra of diatomic molecules (D. Van Nostrand Co. Inc., Princeton, N.J.).
HERZBERG, G. and LAGERQVIST, A. 1968. Can. J. Phys. 46, 2363.
HUO, W. M. 1965. J. Chem. Phys. 43, 624.
———1966. J. Chem. Phys. 45, 1554.
HUBER, M. 1964. Helv. Phys. Acta, 37, 329.
JUNGEN, C. and MIESCHER, E. 1969. Can. J. Phys. 47, 1769.
KRISHNAMACHARI, S. L. N. G. and SINGH, M. 1965. Current Sci. (India), 34, 655.
KRUPENIE, P. H. 1966. The band spectrum of carbon monoxide (National Bureau of Standards Publication NSRDS–NBS 5, Washington, D.C.).
LEFEBVRE-BRION, H. and MOSER, C. M. 1965a. J. Mol. Spectry. 15, 211.
——— 1965b. J. Chem. Phys. 43, 1394.
LEFEBVRE-BRION, H., MOSER, C. M., and NESBET, R. K. 1964. J. Mol. Spectry. 13, 418.
LOFTHUS, A. 1960. The Molecular Spectrum of Nitrogen, Spectroscopic Report No. 2, Department of Physics, University of Oslo, Blindern, Norway.
LUTZ, B. 1969. J. Chem. Phys. 51, 706.
MACDONALD, J. K. L. 1932. Proc. Roy. Soc. (London), Ser. A, 138, 183.
MAL'TSEV, A. A. 1960. Opt. Spectry. 9, 225; Opt. i Spektroskopiya, 9, 428.
MULLIKEN, R. S. 1960. J. Chem. Phys. 33, 247.
MURAD, E., HILDENBRAND, D. L., and MAIN, R. P. 1966. J. Chem. Phys. 45, 263.
NESBET, R. K. 1964. J. Chem. Phys. 40, 3619.
——— 1965. J. Chem. Phys. 43, 4403.
ONAKA, R. 1957. J. Chem. Phys. 27, 374.
PEARSE, R. W. B. and GAYDON, A. G. 1963. The identification of molecular spectra, 3rd ed. (Chapman and Hall, London).
ROBINSON, D. W. 1963. J. Mol. Spectry. 11, 275.
TILFORD, S. G. 1969. J. Chem. Phys. 50, 3126.
TILFORD, S. G. and VANDERSLICE, J. I. 1968. J. Mol. Spectry. 26, 419.